

Reprinted from

# Trends in Solid Mechanics 1979

Proceedings of the Symposium dedicated to  
the 65th Birthday of W.T. Koiter

Delft University of Technology  
June 13 - 15, 1979

J.F. Besseling/A.M.A. van der Heijden/*editors*

Delft University Press  
Sijthoff & Noordhoff International Publishers  
1979

# Buckling: Progress and Challenge

*B. Budiansky and J.W. Hutchinson\**

## Summary

The general theories of elastic and plastic buckling and post-buckling behavior of structures are summarized briefly, and several special topics of current interest are discussed.

## 1. Introduction

It is tempting to begin this survey of the subject of buckling with a long backward look at its history and to muse on the special fascination it has held for so many engineers and scientists. Everybody loves a buckling problem! Without sentimentality, however, we will limit ourselves to the simple but confident introductory assertion that great progress in the understanding of buckling phenomena has been achieved in the last four decades. It is symptomatic of the vigor of the subject that surveys, assessments, and recapitulations of this progress have been appearing with unusual frequency [e.g. 1, 2, 3]. Nevertheless, we welcome with pleasure this opportunity to present our own overview at this symposium in honor of the central contemporary figure in the field of buckling and stability of structures, Warner Koiter.

With deference to the fact that we face a mixed audience of specialists and non-specialists we will try not to get too technical as we summarize progress, outline solutions, and pose problems. To set the stage, we shall give a succinct précis of some of the main concepts and results of general elastic buckling theory, and then describe several of the mode-interaction problems that have recently been under scrutiny by various investigators. We will turn next to a description of the far less well appreciated results of the general theory of plastic buckling and post-buckling behavior, focus on some central unsolved basic problems, and indicate current attempts to reach acceptable solutions. Finally, we will conclude with some observations, necessarily brief, on several related topics that have engaged the attention of the buckling community, including optimum design, stochastic buckling, and the unresolved, nagging problem of the quest for a basic, general stability theorem.

## 2. General Theory of Elastic Buckling

The general theory of elastic buckling and post-buckling behavior was presented by Koiter in his 1945 Ph.D. thesis [4]. After a dormant period of over fifteen years the basic ideas of the

\* Division of Applied Sciences, Harvard University, Cambridge, Massachusetts 02138, U.S.A.

theory started to become widely known, and by now have been the subject of numerous alternative (but essentially equivalent) expositions [3, 5-7]. The theory has found applications to many specific problems and, indeed, informs all current understanding of buckling phenomena. We shall summarize briefly some essential features of the general theory, in a functional notation [3] that, while not in common use, is succinct, general and convenient for applications.

In the study of the equilibrium displacements  $u$  produced in an elastic body by prescribed loads proportional to a scalar measure  $\lambda$ , it is convenient to introduce an inner-product functional  $\langle u, v \rangle$  and a norm  $\|u\| = \langle u, u \rangle^{1/2}$ . We suppose the existence of a *fundamental* displacement  $u_0(\lambda)$  that varies continuously from  $\lambda = 0$  (see Fig. 1(a)), and contemplate the possibility that a distinct equilibrium path

$$u = u_0(\lambda) + v(\lambda) \quad (2.1)$$

sprouts from the fundamental path at the critical load  $\lambda = \lambda_c$ . The normalized *bifurcation* mode may be defined by

$$u_1 = \lim_{\lambda \rightarrow \lambda_c} v / \|v\| \quad (2.2)$$

and then, with the introduction of the scalar parameter

$$\xi = \langle v, u_1 \rangle \quad (2.3)$$

the bifurcated path can be described via the dependence of  $v$  and  $\lambda$  on  $\xi$ . The expansions

$$u = u_0(\lambda) + \xi u_1 + \xi^2 u_2 + \dots \quad (\langle u_n, u_1 \rangle = 0, n \geq 2) \quad (2.4)$$

and

$$\lambda = \lambda_c + \lambda_1 \xi + \lambda_2 \xi^2 + \dots \quad (2.5)$$

may then be used in a standard perturbation procedure for solving the governing equations of equilibrium and thereby deducing  $u_1, u_2, \dots$  and  $\lambda_c, \lambda_1, \lambda_2, \dots$ .

In a conservative elastic system, equilibrium may be enforced by the variational assertion

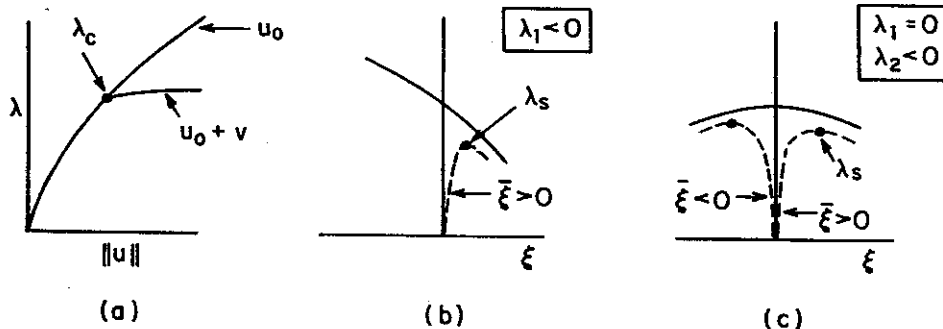


Fig. 1. Bifurcations, imperfections, limit points.

$$\delta\phi = \phi' [u; \lambda] \delta u = 0 \quad (2.6)$$

where  $\phi$  is the potential energy functional of the system, the prime denotes Fréchet differentiation, and  $\delta u$  is an arbitrary admissible variation of displacement. Either (2.6), or its Euler-equation consequences, may serve as the vehicle for the generation of a hierarchy of governing equations of various orders in  $\xi$  that follow from the expansions (2.4) and (2.5). If (2.6) is used, the result is:

$$\begin{aligned} \xi [\phi_c'' u_1] \delta u &= 0 \\ + \xi^2 [\phi_c'' u_2 + \lambda_1 \phi_c'' u_1 + \frac{1}{2} \phi_c''' u_1^2] \delta u &= 0 \\ + \xi^3 [\phi_c'' u_3 + \lambda_1 (\phi_c'' u_2 + \phi_c'' u_1^2) + \lambda_1^2 (\frac{1}{2} \phi_c''' u_1^2) \\ + \lambda_2 \phi_c'' u_1 + \phi_c''' u_1 u_2 + \frac{1}{6} \phi_c^{iv} u_1^3] \delta u &= 0 \\ + \dots &= 0 \end{aligned} \quad (2.7)$$

where  $\phi_c^{(n)} \equiv \phi^{(n)} [u_0(\lambda_c), \lambda_c]$  and  $(\cdot) \equiv \frac{\partial}{\partial \lambda}(\cdot)$ .

The perturbation equilibrium equation of order  $\xi$  provides a homogeneous problem for the lowest eigenvalue  $\lambda_c$  and the corresponding eigenfunction  $u_1$ , and if the solution for  $u_1$  is unique (except for sign) the perturbation procedure is unambiguous. In this single-mode case, setting  $\delta u = u_1$  in the equilibrium equation of order  $\xi^2$  gives

$$\lambda_1 = \frac{1}{2} \phi_c''' u_1^3 / (-\phi_c'' u_1^2) \quad (2.8)$$

and if  $\lambda_1 = 0$ , a similar calculation with the third-order equation yields

$$\begin{aligned} \lambda_2 &= (\frac{1}{6} \phi_c^{iv} u_1^4 + \phi_c''' u_1^2 u_2) / (-\phi_c'' u_1^2) \\ &= (\frac{1}{6} \phi_c^{iv} u_1^4 - \phi_c'' u_2^2) / (-\phi_c'' u_1^2) \end{aligned} \quad (2.9)$$

(Stability considerations imply positive values for the denominators of (2.8) and (2.9).)

If  $N$  linearly independent eigenfunctions  $u_{1i}$  are found at  $\lambda_c$ , they may be orthonormalized ( $\langle u_{1i}, u_{1j} \rangle = \delta_{ij}$ ) and the expansion (4) may be modified to

$$u = u_0(\lambda) + \sum_{i=1}^N \xi_i u_{1i} + \sum_{i=1}^N \sum_{j=1}^N \xi_i \xi_j u_{2ij} + \dots \quad \langle u_{2ij}, u_{1k} \rangle = 0 \quad (2.10)$$

where  $\xi_i = \langle v, u_{1i} \rangle$  and  $\xi^2 = \sum_{i=1}^N \xi_i \xi_i$ . In turn, each  $\xi_i$  is expanded in powers of  $\xi$ , which is now intrinsically positive. Then perturbation equations of successive order provide information for the determination of admissible bifurcation modes specified by  $\nu_i = \lim_{\lambda \rightarrow \lambda_c} \xi_i / \xi$ , the corresponding values of  $\lambda_1$ , and, if necessary, the  $u_{2ij}$  and  $\lambda_2$ .

The major significance of the quantities  $\lambda_1$  and  $\lambda_2$  is their implication concerning *imperfection sensitivity*. If, in the single-mode case,  $\lambda_1 \neq 0$ , or if  $\lambda_1 = 0$  and  $\lambda_2 < 0$ , small initial geometrical imperfections will generally induce snap buckling at loads  $\lambda_s$  smaller than  $\lambda_c$  (see Fig. 1(b, c)). (The same is true for the multi-mode case, except that, since  $\xi$  is then intrin-

sically positive,  $\lambda_1 > 0$  does not necessarily imply imperfection sensitivity.) Explicit asymptotic formulas for  $\lambda_s$  can be found on the basis of a modified potential  $\bar{\phi}[u, \bar{u}]$  valid when an initial displacement  $\bar{u}$  is present. Thus, for the special case of a *linear fundamental state*, in which  $u_0(\lambda)$  is proportional to  $\lambda$ , the *knockdown-factors*  $\lambda_s/\lambda_c$  are:

$$\lambda_s/\lambda_c \approx 1 - 2 \left( -\frac{\lambda_1 \bar{\xi}}{\lambda_c} \right)^{1/2} \quad (\lambda_1 \bar{\xi} < 0) \quad (2.11)$$

$$\lambda_s/\lambda_c \approx 1 - 3 \left( -\frac{\lambda_2 \bar{\xi}^2}{4\lambda_c} \right)^{1/3} \quad (\lambda_1 = 0, \lambda_2 < 0) \quad (2.12)$$

where

$$\bar{\xi} = \langle \bar{u}, u_1 \rangle \quad (2.13)$$

is the 'amount' of bifurcation mode  $u_1$  contained in an initial imperfection  $\bar{u}$ . The same formulas apply in the multi-mode case if  $\bar{u} = \sum_{i=1}^N \nu_i u_{1i}$  is in the shape of one of the bifurcation modes. A method for deducing the influence of initial imperfections in the shapes of a few *nearly* coincident eigenmodes  $u_{1i}$  is to use the expression (2.10) directly in the variational equation

$$\delta \bar{\phi}[u, \sum \bar{\xi}_i u_{1i}] = 0 \quad (2.14)$$

and thereby deduce approximate relations among  $\lambda$ , the displacement measures  $\xi_i$ , and the imperfection parameters  $\bar{\xi}_i$ . In some problems only the terms of order  $\bar{\xi}_i$  will be needed; in others the quadratic terms are necessary, and then the  $u_{2ij}$  can be chosen in the forms they *would* have had if the modes were actually coincident [21]. More about this later.

The importance of the results (2.11) and (2.12) is that they offer a rational explanation for the inability of many structures (particularly shells) to achieve their ideal buckling strengths: they demonstrate the sensitivity of their actual strengths to initial imperfections, and they provide useful quantitative estimates for the magnitude of this sensitivity. We should also mention the significant fact, emphasized by Koiter, that the equilibrium along the descending portions of the curves in Fig. 1(b, c) is *unstable*. Numerous references to specific problems that have been solved by application of the general theory are contained in the surveys [1], [8], and [9].

### 3. Mode Interaction Problems

Despite the apparent special character, from a mathematical viewpoint, of multiple-eigenvalue problems, practical situations in which several bifurcation modes interact must be considered frequently. There is a fundamental reason for this: optimum design tends to produce structures having nearly equal resistances to more than one mode of failure. There are two well-known primitive structural systems — the spherical shell under external pressure and the circular cylindrical shell under axial stress — that are already, in a sense, optimum, and have a large number of independent bifurcation modes at, or very close to, the lowest

bifurcation load. The notorious imperfection-sensitivity of these shells has been studied extensively, and although unresolved questions remain, these problems will not be addressed here. Rather, we shall direct our attention to recent attempts to understand mode-interaction problems of column, plate, and shell assemblies that are designer-induced by the quest for optimality.

The model structure shown in Fig. 2(a) captures many of the characteristic features of mode-interaction phenomena. It consists of an assembly of two elementary spring-supported structures, with the little component providing support to the big one. The strain-energy functions for the restraining springs are taken as

$$\mathcal{E}_z = l \left[ \frac{z^2}{2} + \frac{Bz^4}{4} \right] \quad (3.1a)$$

$$\mathcal{E}_y = \lambda_E \left[ \frac{y^2}{2} + \frac{Ay^4}{4} \right] \quad (3.1b)$$

respectively. The special choices  $B = \pm 1$ ,  $A = \pm 1$  lead to the familiar initial post-buckling behaviors sketched in Fig. 2(b, c) for the two components considered as separate structures.

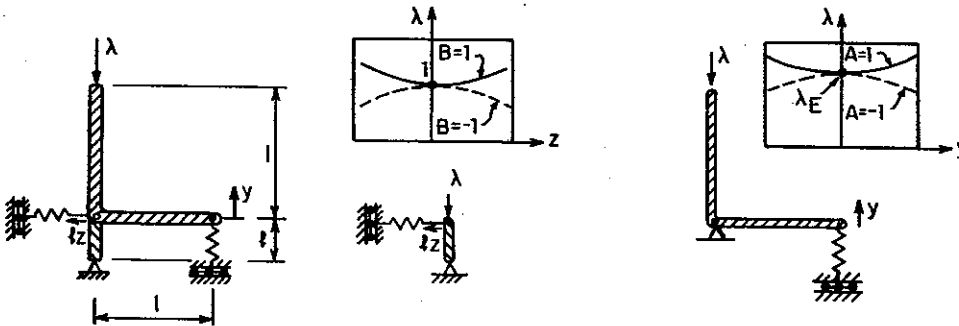


Fig. 2. Mode-coupling model.

For the combined structure of Fig. 2(a) the governing potential energy functional (to fourth-degree terms) is

$$\phi = \mathcal{E}_z + \mathcal{E}_y - \lambda \left\{ l \left[ \frac{z^2}{2} (1+y) + \frac{z^4}{8} (1+l) \right] + \frac{y^2}{2} + \frac{y^4}{8} \right\} \quad (3.2)$$

and from the equilibrium conditions  $\frac{\partial \phi}{\partial z} = \frac{\partial \phi}{\partial y} = 0$  a rich variety of behaviors emerge.

For the sake of future analogy, we dub  $z$  and  $y$  the displacements corresponding to *local* and *overall* modes, respectively. The associated buckling loads of separate structures are 1 and  $\lambda_E$ . These remain the two critical loads for the combined structure, with the post-buckling behaviors sketched in Fig. 3 for the case  $A = B = 1$  and  $l = 1/4$ . For  $\lambda_E < 1$  the lowest bifurcation is stable, but a secondary bifurcation at  $\lambda = \lambda_g$  lurks in its vicinity. Furthermore,

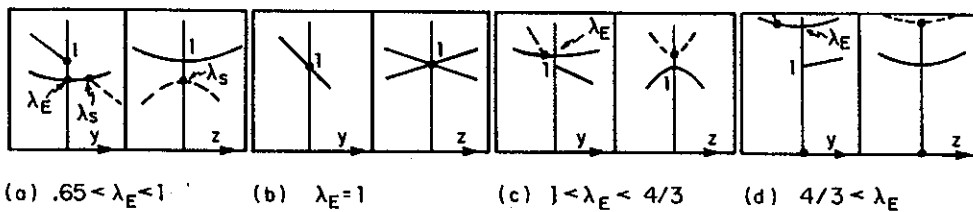


Fig. 3 Mode-interaction behavior of model ( $A = B = 1$ ).

this secondary bifurcation is unstable for  $\lambda_E > .65$ . When  $\lambda_E = 1$ , so that the lowest eigenvalue is a multiple one, an unstable mode reveals itself right at bifurcation, and instability of the fundamental mode persists up to  $\lambda_E = 4/3$ . For  $\lambda_E > 4/3$ , the critical mode is once more stable, but now no secondary bifurcation, unstable or not, exists in the vicinity of the buckling load  $\lambda = 1$ . (In this range determination of the maximum load of the perfect model structure would depend on higher order terms in the potential energy, not taken into account in the present analysis.)

Analogous results could be sketched for other combinations of  $A$  and  $B$  corresponding to unstable post-buckling behavior of one or both of the individual structures. Further, the effects of initial imperfections in  $y$  or  $z$  or both can be assessed. A small sampling of the kinds of results obtainable is exhibited in Fig. 4. In this figure stable bifurcations are denoted by solid lines, unstable ones by dashed lines, and limit-point buckling by dotted lines. The various behaviors of Fig. 3 for the perfect structure, with  $A = B = 1$ , correspond to Fig. 4(a), which also shows results for an imperfection  $\bar{y} = .01$  in the overall mode. The imperfection-sensitivity in the neighborhood of  $\lambda_E = 1$  is evident. The results in Fig. 4(b) (imperfection-sensitive overall mode) and Fig. 4(c) (both modes imperfection-sensitive) display enlarged domains of imperfections-sensitivity, but it is notable that near  $\lambda_E = 1$  the magnitudes of the knockdown factors are not much dependent on  $A$  and  $B$ , at least for the very small imperfection considered. In other words, even if the decoupled structures are individually imperfection-insensitive, they can interact unstably, and near  $\lambda_E = 1$  they may do so in a way that is not changed very much by the introduction of imperfection-sensitivity into the decoupled structures.

Two underlying mechanisms of unstable mode interaction are evident from our model; they may conveniently be characterized as *load amplification* and *support degradation*. Thus

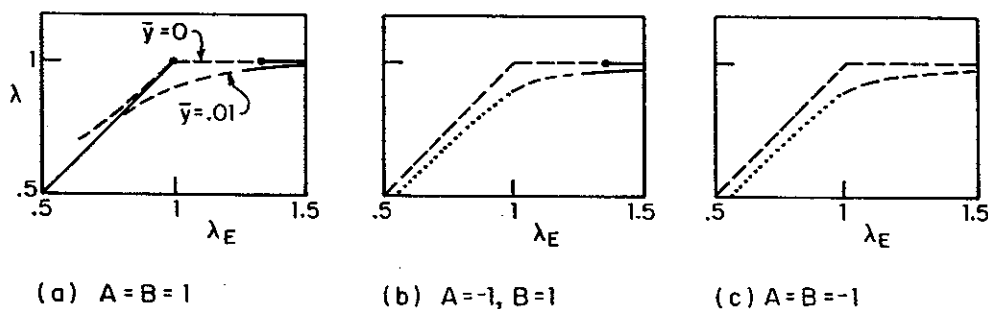


Fig. 4. Stable bifurcations (—), unstable bifurcations (---), limit points (...).

(see Fig. 2(a)) a positive displacement  $y$  in the overall mode makes the load applied to the local supporting structure greater than  $\lambda$ . On the other hand, a displacement  $z$  in the local mode reduces the effective support supplied to the primary structure at the juncture of the two components. These two basic mechanisms of mode interaction can be recognized in the more realistic structures to which we turn next.

Each of the structures shown in Fig. 5 has received detailed analysis during the last decade, and each involves the interaction of recognizable local and overall modes. The lattice column [7, 10] displays interaction between overall Euler buckling and the local buckling of the vertical members as columns over many supports. Here there is negligible post-buckling increase of load associated with both the individual modes, corresponding to essentially neutral stability of each. The two-flange column [11-14] and the wide, stiffened-plate column [15-20] both permit local, multi-wave, plate-element buckling (stable) to interact with overall Euler buckling (neutral). Finally, the axially loaded, longitudinally stiffened cylinder [21, 22] permits interaction between local, longitudinally multi-wave, interstiffener skin buckling (either stable or unstable) and an overall, circumferentially multi-wave, skin-stiffener mode (usually unstable). In each problem-type, unstable mode interaction occurs, with results that are often remarkably similar to those displayed by our simple two-degree-of-freedom model. We will not exhibit these special results, but a qualitative discussion of various lines of attack on the problem of Fig. 5 may be of some interest.

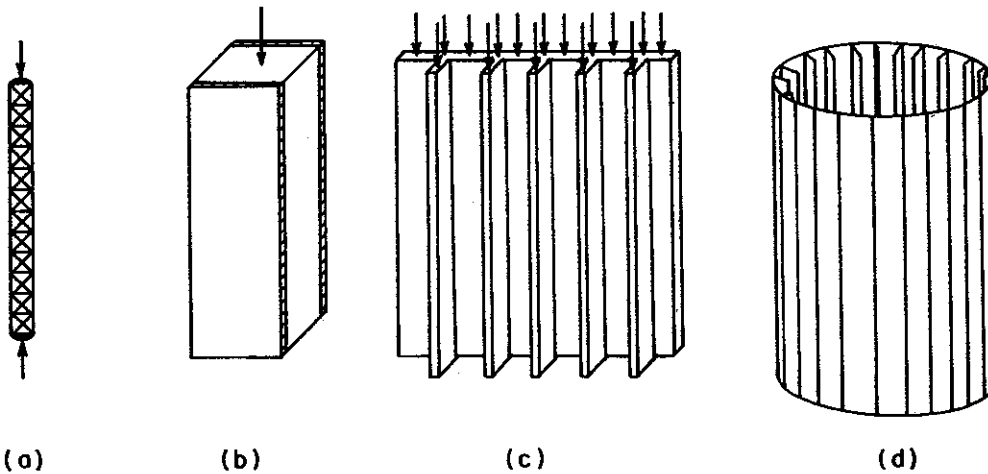


Fig. 5. Mode-interacting structures.

Three different approaches have been made. The first (and oldest) analyzes the decoupled local buckling behavior, and then presents to the overall structure an associated degraded local support stiffness. The coupling mechanism of load amplification is thereby also taken into account, because overall deformations will automatically induce forces that drive the local buckling. This approach goes back, at least in concept if not execution, to the early thirties and effective-width ideas. Thus, in the lattice column, the axial stiffnesses of the vertical members are computed as functions of local load and initial local imperfection, and used for the estimation of reduced bending stiffness in an overall column buckling analysis [7, 10]. Similar use has been made of the effective overall bending stiffness supplied by



locally buckled flanges (Fig. 5(b)) [11-13] and buckled plate assemblies (Fig. 5(c)) [17, 20]. (In [19] Koiter and Pignataro show how to make rapid engineering estimates of the effective post-buckling stiffnesses of various kinds of plate assemblies.) But this approach has at least two apparent deficiencies. First, it does not seem to fit comfortably into the framework of the general theory, and so appropriate measures for improvements on its results are not obvious. Second, there is a conceptual flaw in the use of an effective local stiffness as a truly local property in the overall buckling phenomenon, because the local buckling deformations along the length of the structure are not decoupled from each other, as is implicitly assumed when the local stiffnesses are considered to depend only on the local loads. Both objections are met by the approaches taken in [15, 16] for the stiffened panel problem, and in [21] for the stiffened cylinder problem, which are based essentially on the use of the expansion (2.10) in the variational Eq. (2.14) of the general theory, and take into account two, nearly coincident buckling loads, with their associated buckling modes. But the story can not end there. In the problems illustrated in Fig. 5 there may be *many* local buckling modes with nearly equal buckling loads, and local buckling deformations in various parts of the overall structure may be nearly decoupled from each other. The consequence is that the first approach may, after all, be more nearly correct, since the more formal second method embodies only a single local buckling mode. This dilemma has been resolved by Koiter et al [14, 18, 19, 22] in a series of papers that presents the third approach, containing the technique of *amplitude modulation*. Here the apparatus of the general theory is invoked, but now the amplitude of the local buckling mode is permitted to vary from point to point in the overall structure. This is not rigorous, but provides an effective recognition of the existence of many local modes having nearly the same critical loads. Not only does the approach recapture the results of the earlier local-effective-stiffness methods, it points the way toward useful extensions to other problems.

In recent work Koiter and van der Neut [23] come to grips with mode interaction problems wherein several local modes that do *not* share nearly equal critical loads play an essential role. This occurs, for example, in the intriguing problem of the interactive buckling of a long square tube of uniform thickness. An elementary explanation of the mode-coupling involved can be seen with the help of Fig. 6. Plate bending  $w$  produces longitudinal strains proportional to  $w^2$ . Accordingly, combining the strains due to overall bending (proportional to  $z$ ) with those due to plate buckling leads to a strain energy contribution per unit column length given approximately by

$$\oint [c_1 z + (c_2 w_1 + c_3 w_2)^2]^2 ds \quad (3.3)$$

where the coefficients  $c_1, c_2, c_3$  are proportional to the amplitudes of the modes in overall (Euler) buckling and the two plate modes shown in Fig. 6(a) and 6(b). The consequence is that the only overall-local coupling term that survives the symmetry of the cross-section is

$$4c_1 c_2 c_3 \oint (z w_1 w_2) ds \quad (3.4)$$

and so the mode interaction phenomenon would be completely missed if the mode types in either Fig. 6(a) or Fig. 6(b) were omitted from the analysis.

What of the future? While the studies of the last ten years have produced much understanding, and clever approximate analyses have swept away some seemingly complicated computational barriers, our feeling (shared with Tvergaard [1]) is that the subject of mode interaction in practical structures may be ripe for brutal computerization. Given the nearly

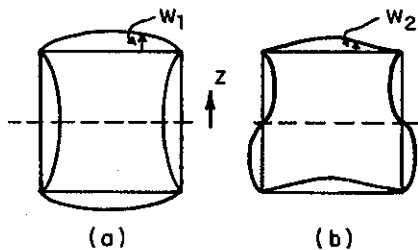


Fig. 6. Plate modes in square tube.

routine but sophisticated computer capabilities that now exist for the calculation of bifurcation loads and modes (e.g. [24-26]) and the theoretical foundations provided by the general theory of post-buckling behavior, it does not seem too optimistic to expect that a concerted effort would produce powerful, multi-mode computer procedures for the assessment of mode interaction in column, plate, and shell assemblies.

#### 4. Plastic Buckling

Compared to elastic buckling, plastic buckling is an underdeveloped subject. Conditions for bifurcation are well established, and some fairly general results characterizing behavior immediately following bifurcation are known. But a general understanding of post-bifurcation behavior and imperfection-sensitivity in the plastic range does not yet exist. Here an attempt will be made to survey broadly various pieces of the subject which are understood and to point to aspects on which progress may be possible. We recognize that numerical methods are indispensable for solving practical plastic buckling problems, even more so than for elastic buckling. Nevertheless, the absence of a theory of plastic buckling and post-buckling behavior leaves the subject at the present as little more than a collection of rather unrelated example problems.

##### 4.1. Bifurcation in the plastic range

Shanley's [27] rationalization of the tangent modulus load for compressed columns has been generalized for elastic-plastic continua by Hill [28]. Some of the unresolved issues related to choice of constitutive law will be touched upon below. Irrespective of these issues, Hill's formulation embraces most plasticity laws of conceivable interest in buckling. It is fair to say that the mathematical aspects of the bifurcation problem for the lowest bifurcation load are well founded, apart from a difficulty analogous to that in elastic buckling related to sufficiency conditions for stability. Hill's theory has now gained wide-spread acceptance. Sewell [29] has reviewed Hill's theory and has related it to earlier buckling work. Sewell's article contains an organized list of over 600 references on plastic buckling. More recent survey reports of limited circulation have been prepared by Sewell [30] and Storåkers [31]. Tvergaard's survey [1] covers aspects of plastic buckling and post-buckling.

As in the elastic case the fundamental solution whose uniqueness is in question,  $u_0(\lambda)$ , is

assumed to be a function of a single load or deformation parameter  $\lambda$  which increases from zero. Bifurcation from the fundamental solution is assumed to occur prior to the occurrence of a limit point in  $\lambda$ . On the bifurcated branch we consider monotonic growth of the bifurcation mode.

Hill [28] introduces a quadratic functional of the displacement-rate for testing for bifurcation. The instantaneous moduli which enter into this functional are called comparison moduli. Loosely speaking, at each point in the body the comparison moduli are the softest branch of available moduli at that state. With a smooth yield surface, the comparison moduli are simply the plastic loading moduli wherever the stress is at yield, and the instantaneous elastic moduli elsewhere. The situation is more complicated when the stress is at the corner of a yield surface. If a total loading regime exists (i.e., a range of stress-rates in which all potential active yield systems are actually activated), then the comparison moduli are the total loading moduli. Bifurcation is first possible at the load  $\lambda_c$  where the quadratic functional vanishes for a non-zero admissible displacement-rate.

#### 4.2 Post-bifurcation behavior

The search for the lowest bifurcation load has been reduced to a standard eigenvalue problem subject to the constraint that bifurcation does occur in such a way that the comparison moduli *are* activated by the bifurcation mode. It is this constraint which gives rise to bifurcation under increasing load and which determines the linear combination of the eigenmode and the fundamental solution increment comprising the bifurcation mode. We will use an axially compressed, simply supported column to illustrate initial post-bifurcation behavior.

The slender, solid cylindrical column shown in Fig. 7 has been analyzed within the framework of the approximations of simple column theory (Hutchinson [32]) wherein strain-rates are assumed to be linearly distributed through the thickness and the stress is taken to be uniaxial at each point. Later we will comment on the relation of these results to a more accurate 3-dimensional analysis.

The lowest bifurcation load (Shanley's tangent modulus load) is

$$\lambda_c = \pi^2 E_t^c I / L^2 \tag{4.1}$$

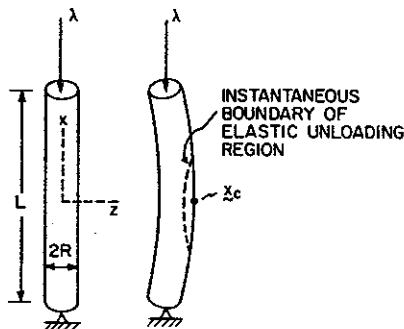


Fig. 7. Simply supported column with solid circular cross-section.

where  $I$  is the moment of inertia of the cross-section and  $E_t^c$  is the tangent modulus of the uniaxial stress-strain curve at the bifurcation stress. The lateral deflection component of the eigenmode is

$$w_1 = R \cos \left( \frac{\pi x}{L} \right) \quad (4.2)$$

The amplitude of the eigenmodal contribution to the total lateral deflection  $w$  is denoted by  $\xi$  so that, by definition,

$$w = \xi w_1 + \tilde{w} \quad (4.3)$$

where  $\tilde{w}$  is orthogonal to  $w_1$ .

Before discussing the behavior of the elastic-plastic column, it is revealing to discuss the behavior of a fictional comparison column with elastic unloading suppressed. This makes the column, effectively, nonlinearly elastic, and it can then be analyzed by the methods discussed earlier. The lowest bifurcation load is still given by (4.1) with the same eigenmode (4.2). The initial post-bifurcation response is necessarily symmetric in  $\xi$ , and the expansion (2.5) has the form

$$\lambda = \lambda_c + \lambda_2^e \xi^2 + \dots \quad (4.4)$$

where the superscript  $e$  labels quantities limited to the comparison nonlinear elastic column. The post-bifurcation coefficient  $\lambda_2^e$  depends on the first and second derivatives of the tangent modulus at  $\lambda_c$ ; it may be positive or negative. Regardless of the sign of  $\lambda_2^e$ , strain-rate reversal occurs over the entire half of the nonlinear elastic column towards which the lateral deflection takes place. As is well known, a nonlinear elastic column ceases to behave like an elastic-plastic column as soon as bifurcation occurs.

Bifurcation of the actual elastic-plastic column must take place under increasing load in such a way that the tangent modulus  $E_t$  governs the response everywhere in the column. With

$$\lambda = \lambda_c + \lambda_1 \xi + \dots,$$

the stress immediately following bifurcation is

$$\sigma = \sigma_0^c + \xi(\lambda_1 \dot{\sigma}_c + \sigma_1) + \dots \quad (4.5)$$

where  $\dot{\sigma}_c = (\partial \sigma_0 / \partial \lambda)_c$  and  $\sigma_1$  is the eigenmodal contribution. The constraint that plastic loading occurs everywhere in the column as  $\xi$  increases from zero requires

$$\lambda_1 / \lambda_c \geq 4. \quad (4.6)$$

On the other hand, if  $\lambda_1 / \lambda_c > 4$  then, by continuity, no elastic unloading occurs in some finite neighborhood of  $\lambda_c$ . But this is not possible since then, for sufficiently small  $\xi$ , (4.4) would hold giving rise to immediate unloading over half the column. Elastic unloading must start at bifurcation with  $\lambda_1 / \lambda_c = 4$ . In other words, the bifurcation mode, which is the combination of the fundamental solution-rate and the eigenmode of order  $\xi$  in (4.5), must

satisfy neutral loading somewhere in the body. For the column problem this translates into

$$\max(\lambda_1 \dot{\sigma}_c + \sigma_1) = 0 \quad (4.7)$$

which leads to  $\lambda_1/\lambda_c = 4$ . For the column with the solid circular cross-section there is exactly one point  $x_c = (R, 0, 0)$  where (4.7) is attained, assuming without loss in generality,  $\xi > 0$ . This point is indicated in Fig. 7. Elastic unloading spreads from  $x_c$  as  $\xi$  increases. The next term in the initial post-bifurcation expansion reflects the growth of the elastic unloading region. The general form of the initial post-bifurcation expansion, for the column and more general situations, is [32, 33]

$$\lambda = \lambda_c + \lambda_1 \xi + \lambda_2 \xi^{1+\beta} + \dots \quad (4.8)$$

where  $\beta$  depends on the geometry in the neighborhood of  $x_c$ . The general formula for  $\lambda_2$  depends only on the bifurcation mode. For the column of Fig. 7,

$$\beta = \frac{1}{3} \quad \text{and} \quad \frac{\lambda_2}{\lambda_c} = -3 \left\{ \frac{3\pi E_t^c}{E - E_t^c} \left[ 1 + \left( \frac{\pi R}{2L} \right)^2 \left( \frac{dE_t}{d\sigma} \right)_c \right] \right\}. \quad (4.9)$$

The lowest order equation for the surface separating the spreading lens-shaped zone of elastic unloading from the plastically loading region is

$$(R-z)/R + \frac{1}{2} (\pi x/L)^2 = \frac{1}{3} (-\lambda_2/\lambda_c) \xi^{4/3}. \quad (4.10)$$

The above results were also obtained from an approximate 3-dimensional analysis [33], except that  $\lambda_2$  is then a weak function of Poisson's ratio which agrees with (27) in the limit of incompressibility. In the 3-dimensional treatment a boundary layer analysis is used to obtain the lowest order equation (4.10) governing the growth of the unloading region. Because of the presence of the negative term  $\lambda_2 \xi^{4/3}$  in (4.8), the rate of increase of the load following bifurcation is rapidly eroded. This explains why the maximum support load is often only slightly above  $\lambda_c$  in spite of a large initial rate of load increase. From (4.10) it can be seen that the unloading region rapidly encroaches on the column. In the general case the rate at which elastic unloading makes its presence felt in the expansion (4.8) through the term  $\lambda_2 \xi^{1+\beta}$  depends on the geometry in the neighborhood of the point, or set of points, at which elastic unloading starts. Several other examples are shown in Fig. 8.

Tvergaard and Needleman [34, 35] have studied several examples where structural asymmetry results in post-buckling behavior in the plastic range which is entirely different from that in the elastic range. A good example is the simply supported column with a solid, equilateral triangular cross-section shown in Fig. 8 and again in Fig. 9.

Within the framework of column theory a linearly elastic column has a symmetric buckling behavior even though the cross-section is asymmetric. This is not the case for a comparison nonlinearly elastic column [34]. For buckling about the  $y$ -axis,

$$\lambda = \lambda_c + \lambda_1^e \xi + \dots \quad (4.11)$$

where

$$\frac{\lambda_1^e}{\lambda_c} = \frac{8\sqrt{2}}{15\pi} \frac{q}{1+q} \quad \text{with} \quad q = \frac{1}{18} \left( \frac{\pi h}{L} \right)^2 \left( \frac{dE_t}{d\sigma} \right)_c. \quad (4.12)$$

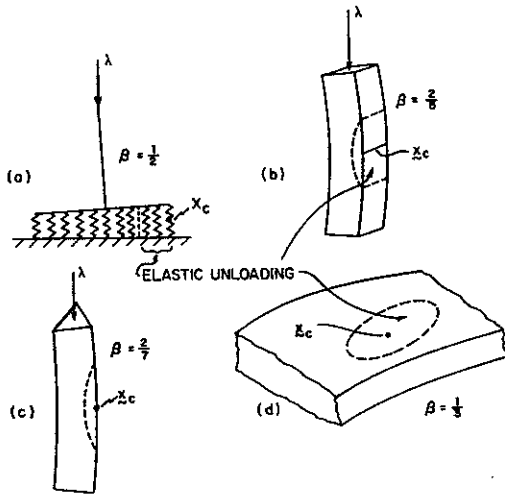


Fig. 8. Onset and spread of elastic unloading region.

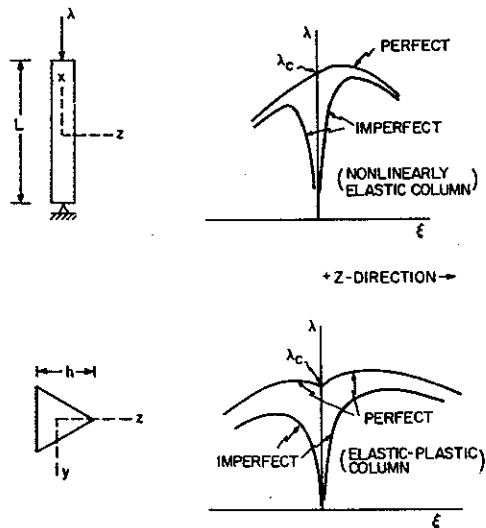


Fig. 9. Buckling of a simply-supported column with solid triangular cross-section about  $y$ -axis.

Here  $\lambda_c$  is given by (4.1) and, instead of (4.2),  $w_1 = (h/2\sqrt{3}) \cos(\pi x/L)$  with  $\xi$  defined by (4.3). For a typical stress-strain curve, with  $E_t$  decreasing as  $|\sigma|$  increases,  $dE_t/d\sigma$  is positive for compression. Then (4.11) implies that the load falls for buckling deflections towards the flat side of the cross section ( $\xi < 0$ ) and increases when buckling occurs towards the point of the triangle ( $\xi > 0$ ) as depicted in Fig. 9.

For the elastic-plastic column

$$\lambda/\lambda_c = 1 + 2\sqrt{2\xi} + (\lambda_2/\lambda_c)\xi^{9/7} + \dots, \quad \xi \geq 0 \quad (4.13)$$

$$\lambda/\lambda_c = 1 + \sqrt{2(-\xi)} + (\lambda_2/\lambda_c)(-\xi)^{7/5} + \dots, \quad \xi \leq 0 \quad (4.14)$$

where expressions for  $\lambda_2$  are given in [34]. The initial rate of increase of load is larger by a factor of 2 for buckling towards the point of the triangular cross-section ( $\xi > 0$ ). Thus the initial post-bifurcation behaviors of both the nonlinearly elastic and the elastic-plastic column indicate a greater reserve of post-buckling strength for buckling with  $\xi > 0$ . A numerical analysis of the column (including effects of initial imperfections) was also carried out by Tvergaard and Needleman. The greater post-buckling resistance for  $\xi > 0$  was indeed verified with findings such as those depicted in Fig. 9.

Using the same set of techniques, Tvergaard and Needleman [35] also investigated the important problem of the buckling of an eccentrically stiffened wide-column such as that shown in Fig. 5(c). The post-buckling strength of the wide column in the plastic range was found to be the greatest for buckling towards the side of the column on which the stiffeners are attached. The column is significantly less sensitive to imperfections which promote buckling towards the stiffeners compared to those which cause deflections in the opposite direction.

While the initial post-bifurcation expansion (4.8) gives insight into how the rate of load increase diminishes so rapidly following bifurcation, it does not usually provide a means of accurately predicting the maximum load and the associated buckling deflection. Van der Heijden [36] has proposed an alternative approximate analysis aimed at predicting the maximum load of a structure with or without imperfections. The simple continuous spring model of Fig. 8 was used to try out the approach.

With reference to Fig. 10, let  $\lambda_c$  denote the lowest bifurcation load and let  $\lambda_{rm}$  denote the reduced modulus load of von Karman [37] where bifurcation takes place under constant load to lowest order in  $\xi$ . Using perturbation methods it is possible to determine the expansion of the solution bifurcating at  $\lambda_{rm}$ , i.e.

$$\lambda = \lambda_{rm} + \lambda_2^{rm} \xi^2 + \dots \quad (4.15)$$

Central to van der Heijden's method is the determination of the locus of maxima  $\lambda^*(\xi^*)$  associated with solutions bifurcating in the range  $\lambda_c \leq \lambda \leq \lambda_{rm}$ . An expansion about  $\lambda_{rm}$  gives

$$\lambda^* = \lambda_{rm} + A\xi^* + B\xi^{*2} + \dots \quad (4.16)$$

Van der Heijden approximates the solution associated with bifurcation at the lowest load by

$$\lambda = \lambda_c + \lambda_1 \xi + b\xi^2 + c\xi^3 \quad (4.17)$$

where  $\lambda_1$  is the known initial slope. The coefficients  $b$  and  $c$  are chosen such that  $\lambda(\xi)$  in (4.17) crosses the locus of maxima (4.16) with zero slope and with the same curvature as in (4.15) at maximum load. That is,

$$\frac{d\lambda}{d\xi} = 0, \quad \frac{d^2\lambda}{d\xi^2} = 2\lambda_2^{rm} \quad \text{where} \quad \lambda = \lambda^* \quad \text{at} \quad \xi = \xi^*. \quad (4.18)$$

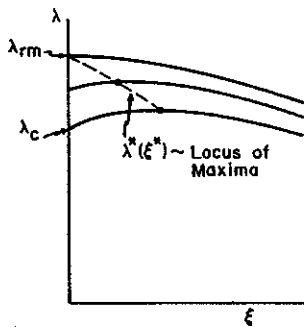


Fig. 10. Bifurcation responses.

In principle, an expansion of the curvature of the solutions, where they cross the locus of maxima, could be developed about  $\lambda_{rm}$  and used to improve the estimate of  $d^2\lambda/d\xi^2$  in (4.18). But this expansion is quite complicated and, by comparison with numerical solutions, van der Heijden found that the curvature at  $\lambda_{rm}$  served as a reasonable approximation. The method was also extended to estimate the effects of small imperfections on the maximum support load.

There is clearly nothing rigorously asymptotic about this method. Indeed, it is unlikely that any purely analytical method can be found to predict the maximum load since it occurs at a finite deflection beyond bifurcation. The method does make use of information which can be determined from expansions about  $\lambda_c$  and  $\lambda_{rm}$ .

Given the history of column buckling, it is interesting that van der Heijden's method brings in Shanley's tangent modulus load and von Karman's reduced modulus load on roughly an equal footing.

#### 4.3. Imperfection-sensitivity

For linearly elastic bodies instability and imperfection-sensitivity derive from geometric nonlinearity. In the plastic range, material nonlinearity in the form of decreasing moduli with increasing deformation is an additional destabilizing influence. In addition, under certain conditions there is an anomalous material-based sensitivity to extremely small imperfections associated with the assumption of a smooth yield surface.

Very few general results are available for the effect of imperfections on the maximum support load in the plastic range. Here we will confine ourselves to the effects of small geometric imperfections of the form  $\xi u_1$ . In many problems of interest the fundamental solution of the perfect structure undergoes no elastic unloading as  $\lambda$  is increased. Elastic unloading starts at bifurcation at  $\lambda_c$  in the manner discussed above. One general result which then holds asymptotically for sufficiently small imperfections is that elastic unloading starts when the slope of the relation between  $\lambda$  and  $\xi$  is reduced to

$$\frac{d\lambda}{d\xi} = \lambda_1 \quad (4.19)$$



where, as in (4.4),  $\lambda_1$  is the initial slope for the perfect structure [38]. The onset of elastic unloading is a pivotal point in any buckling analysis; it is the beginning of inherently irreversible behavior whose effects seem to persist for all larger  $\xi$ .

For problems such as that of the column or the continuous spring model, where the stress history at each point is uniaxial, the value of  $\lambda$  and of  $\xi$  at which elastic unloading starts in the imperfect structure is given by the asymptotic formula for small  $\bar{\xi}$

$$\hat{\lambda} = \lambda_c - C_1 \sqrt{|\bar{\xi}|}, \quad \hat{\xi} = C_2 \sqrt{|\bar{\xi}|}. \quad (4.20)$$

These formulas also hold, in general, for other problems if it is assumed that, prior to elastic unloading, the material is characterized by a deformation theory of plasticity. Formulas for  $C_1$  and  $C_2$ , which depend on the sign of  $\bar{\xi}$ , are given in [32] and [38].

Studies of discrete spring models and of the continuous spring model indicate that the maximum load is also reduced by an amount proportional to the square root of the imperfection for sufficiently small  $\bar{\xi}$ , i.e.

$$\lambda_{\max} = \lambda_{\max}^0 - C_3 \sqrt{|\bar{\xi}|}. \quad (4.21)$$

The strong sensitivity to small imperfections implied by (4.21) is closely connected to the pivotal role of  $\lambda$ . Model studies and numerical studies of more complicated examples show that the maximum load is often attained shortly after the onset of elastic unloading. It has not been shown that (4.21) is precisely valid for other than column-like problems but it seems likely that the asymptotic dependence on the square root of  $\bar{\xi}$  may be a general feature, assuming a smooth yield surface is not used. As will be discussed below, a *much stronger* asymptotic imperfection-sensitivity occurs if bifurcation involves non-proportional plastic loading and if a plasticity theory based on a smooth yield surface is used. We discuss this next. The well-known example of the cruciform column shown in Fig. 11 will be used to illustrate what is involved [39, 40]. For simplicity an incompressible material characterized by  $J_2$  flow (incremental) theory is assumed. The uniaxial stress-strain curve is assumed to be monotonically increasing. The compressive buckling stress of the perfect cruciform associated with torsional buckling is

$$\sigma_c = G(t/b)^2. \quad (4.22)$$

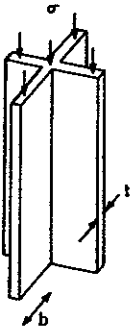


Fig. 11. Cruciform column.

The elastic shear modulus  $G$  governs the incremental shear response in the state of uniaxial compression and consequently controls bifurcation.

The cruciform column is unusual in that bifurcation occurs at constant load, with  $\lambda_1 = 0$ . From (4.19) it follows that elastic unloading in the slightly imperfect column will occur at essentially the maximum load. This observation was exploited in [40] where imperfection-sensitivity was studied with elastic unloading suppressed. The  $J_2$  flow theory with elastic unloading suppressed is an inherently path-dependent hypo-elastic constitutive law. It was found that elastic unloading started just after attainment of the maximum load in the slightly imperfect column if the tangent modulus at bifurcation satisfied  $E_t^c < E/3$ . Thus in this range the maximum load could be calculated using the hypo-elastic characterization.

An asymptotically exact analysis of the equations governing the cruciform was carried out and the asymptotic expression for the maximum load was found to be

$$\lambda_{\max}/\lambda_c = 1 - \mu \bar{\xi}^s. \quad (4.23)$$

Here  $\mu$  is a positive number of order unity which depends on details of the stress-strain curve and

$$s = \frac{E_t^c}{E + E_t^c/2}. \quad (4.24)$$

In the unloaded state the initial imperfection is a twist per unit length  $\bar{\theta}$ ; the nondimensional imperfection amplitude is  $\bar{\xi} = b^2 \bar{\theta}/t$ .

Values of  $s$  less than 1/10 are rather typical for buckling in the plastic range. Therefore, from (4.23) one concludes that an imperfection as small as  $\bar{\xi} = 10^{-10}$  will have a non-negligible influence on the buckling load. This extraordinary sensitivity is due to the hypo-elastic character of the loading branch of  $J_2$  flow theory. It is not restricted to the cruciform column, but can be expected in any problem where bifurcation involves a strongly non-proportional plastic response [28, 41]. The bifurcation load predicted using a flow theory with a smooth yield surface has little meaning when the presence of truly unavoidable imperfections renders it unattainable.

There has been some progress in recent years in developing phenomenological flow theories of plasticity which model incremental behavior at the corner of a yield surface and which are sufficiently simple that they can be used in numerical calculations [42, 43]. These theories can accommodate a description of a nearly-proportional loading response which is the same as that from the  $J_2$  deformation theory of plasticity. Thirty years ago, Batdorf [44] rationalized the use of  $J_2$  deformation theory in bifurcation analyses by appealing to a cornered yield surface. Thus the bifurcation load from one of these theories is the same as that from  $J_2$  deformation theory, which is generally accepted as giving reasonably good estimates of buckling loads when compared with experimental loads. Furthermore, the corner theories will not give rise to a huge sensitivity to unavoidably small imperfections but are likely to display a dependence such as that in (4.21).

Even if sharp corners do not develop at the loading point on a yield surface, a corner theory may be a better model of behavior at a region of high curvature on the yield surface for the purposes of buckling analysis than one of the conventional smooth yield surface theories. If the conventional theory underestimates the local curvature of the yield surface, then it will overestimate the stiffness of the material response for non-proportional loading increments. A corner theory will tend to underestimate this stiffness. Judging from the success of  $J_2$  deformation theory in predicting buckling loads, the corner theory should not be unduly conservative in its buckling predictions.

## 5. Optimum Design

We limit ourselves to three observations:

(1) The alarm was sounded early [45] with respect to the dangers of imperfection-sensitivity in structures having nearly-coincident local and overall buckling loads, with the further speculation that this might vitiate the requirement of critical load coincidence for optimality. Current overviews of the situation tend to confirm the first warning, but not necessarily the second. Optima tend to be smooth, and even if the best design, in the presence of imperfections, is not right at the equal-critical-load configuration, the consequent weight-saving may often be small. But when nearly-coincident critical loads are permitted, adequate knockdown factors must be invoked, and it should be well understood, for whatever inference one might wish to draw concerning the design, that should failure occur at such a design, it is likely to be catastrophic.

(2) An unusually thorough and rigorous optimization study was recently executed by Libai [46], in which an optimum design against elastic buckling (but not failure) was sought for the configuration shown in Fig. 12(a), consisting of a simply-supported square plate containing a central, one-sided, blade stiffener. For a given total end thrust  $P$  and plate dimension  $L$ , the dimensions  $h$ ,  $t_w$ , and  $t_s$  for minimum weight under the constraint of no buckling were sought. Libai found a *local* minimum (in configuration space) at the design for which (a) symmetrical plate-stiffener buckling, (b) uncoupled torsional stiffener buckling, and (c) uncoupled, transversely antisymmetrical plate buckling have very nearly (but not exactly!) the same critical loads. In the practical range of structural index  $P/L^2$ , the stiffener is 'thin' at this configuration, with  $t_w/h$  usually less than 1/10. But a different local minimum, requiring a 'thick' stiffener having  $t_w/h \approx 1/2$ , was also found, providing a design with a very slightly lower weight. The results for  $(\sigma_{cr}/E)$  at the two design minima, shown in Fig. 12(b) as one curve, are indistinguishable on the scale used. The stiffener-to-plate area ratios

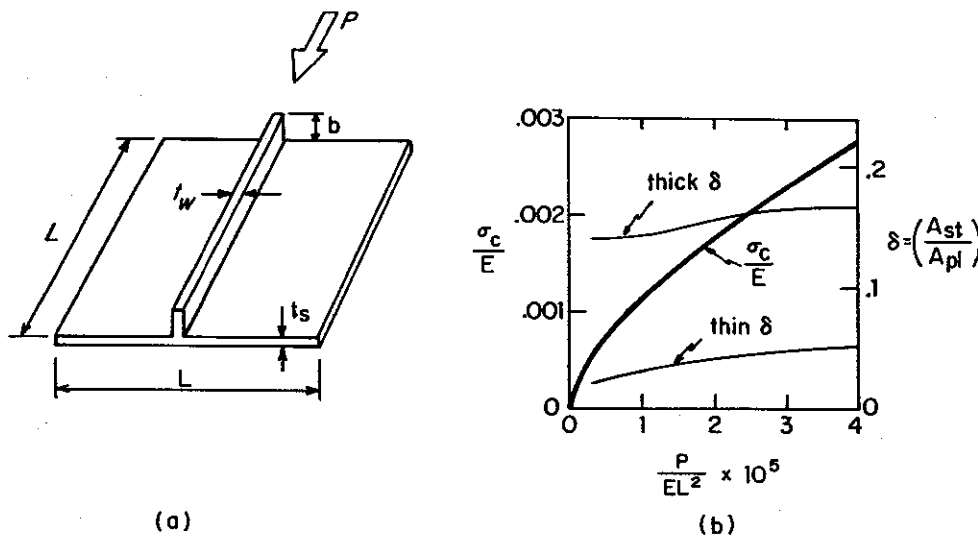


Fig. 12. Centrally-stiffened-plate optima.

are also shown in Fig. 12(b), with very different values at the two optima. At both the thick and thin minima the symmetric mode and the coupled transversely antisymmetric mode had equal buckling loads, but in the case of the thick minimum the stiffener was nowhere near its own torsional instability load. It therefore seems likely that the thick minimum is not imperfection sensitive, but that the thin minimum is. The possibility of finding similar results in the optimum design of other, more realistic configurations should not be overlooked.

(3) It has to be acknowledged that, despite theoretical progress, few practical design optimization problems have, as yet, been 'solved' analytically. In this respect, theory lags experiment, and a glance at a remarkable series of tests conducted over thirty years ago may be instructive [47, 48]. Over 150 2024-ST aluminum alloy zee- and hat-stiffened panels having systematically varied configurations were tested for ultimate compressive strength, with the global results summarized in Fig. 13. Here the appropriate structural index is  $P_i/L\sqrt{c}$ , where  $P_i$  is the load-per-unit-width of panel,  $L$  is the panel length, and  $c$  is an effective end-fixity coefficient ( $c = 1$  for simple support;  $c = 4$  for clamped ends). The curves show the compressive strengths of minimum weight designs. (The actual configurations providing these designs are obtainable from auxiliary curves not shown here.) The most striking feature of these old results is that (at least for equal sheet and stiffener thicknesses) they announce the superiority of zees over hats as stiffeners. These experimental results automatically incorporate the effects of certain representative initial imperfections, not to mention plasticity, discrete rivet attachments, finite corner radii — and they stand as a challenge to theoreticians to confirm or refute them, and deduce analogous results for other configurations and materials.

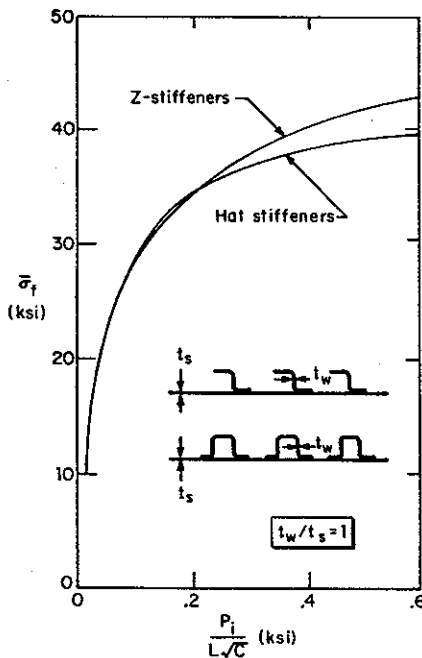


Fig. 13. Optimization of zee- and hat-stiffened panels.

## 6. Stochastic Buckling Problems

Given the importance of small imperfections in imperfection-sensitive structures, and the uncertainty of their magnitudes and shapes, it has long been believed that a rational approach to the design of such structures should relate failure probability under a given loading to appropriate statistical information concerning imperfections. Such correlations are straightforward, in principle, when single-mode buckling is pertinent, for then the probability of failure may be related directly to the probability distribution function of the amplitude of the relevant imperfection. This procedure may be extended when a few modes interact, but becomes cumbersome for many modes. On the other hand, if interacting modes can be idealized into a continuous spectrum, the techniques of generalized harmonic analysis become useful. Examples of the two approaches are contrasted in [49].

The intermediate situation, in which not a few but also not very many modes must be considered to have stochastic imperfections, has been addressed in [50], where the problem of a lattice column with random imperfections in the individual members is tackled. Through the use of effective approximations results for the means and variances of buckling loads are estimated, with accuracies confirmed by Monte Carlo calculations.

## 7. Stability

For some years Koiter has been concerned with a fundamental dilemma in the theory of elastic stability, and has tried to provoke interest in its resolution [51]. Briefly, the situation is this:

Stability is guaranteed at an equilibrium state  $u_0$  if, for some constant  $c$ ,

$$\frac{\Delta\phi}{\|\delta u\|^2} \equiv \frac{\mathcal{E}[u_0 + \delta u] - \phi[u_0]}{\|\delta u\|^2} > c > 0 \quad (7.1)$$

for sufficiently small  $\|\delta u\|$ . This implies that with respect to the assumed norm,  $\phi$  has a strong minimum at  $u_0$ . Subsequent to an initial displacement  $\delta u(0)$  at time  $t=0$  (with velocity  $\delta \dot{u}(0) = 0$ ) energy considerations dictate that with or without damping  $\Delta\phi(t) \leq \Delta\phi(0)$  for all  $t > 0$ . Therefore  $\|\delta u(t)\|$  will never exceed a sufficiently small assigned  $\epsilon$  if the initial restrictions  $\|\delta u(0)\| \leq \epsilon$  and  $\Delta\phi(0) \leq c\epsilon^2$  are imposed. If the choice of norm does not violate our engineering sensibilities, the definition of stability implicit in these facts is acceptable. Trouble arises, however, when, like all good engineers, we propose to replace the sufficient condition (7.1) by the requirement of a positive-definite second variation of the potential energy:

$$\frac{\delta^2\phi}{\|\delta u\|^2} > d > 0 \quad (7.2)$$

where

$$\delta^2\phi \equiv \frac{\partial^2}{\partial \eta^2} [u_0 + \eta \delta u]_{\eta=0} \quad (7.3)$$

(Here the same norm used in (7.1) and (7.2) is invoked in the limit operation involved in the

second derivative). The existence of a continuous second Fréchet derivative  $\phi''$  (which was blithely assumed in [3] and in the first part of this paper) implies the identity

$$\delta^2 \phi = \phi'' (\delta u)^2 \quad (7.4)$$

and then, as Como and Grimaldi [51] have indicated, all is well. For with  $\phi' = 0$ ,  $\Delta \phi = \frac{1}{2} \phi'' (\delta u)^2 + R$ , where  $R/\|\delta u\|^2 \rightarrow 0$  for  $\|\delta u\| \rightarrow 0$ , and then (7.4) and (7.2) imply (7.1), which implies stability. Indeed, by establishing the existence of Fréchet derivatives with respect to suitable norms Como and Grimaldi [53] verify Koiter's proof [54] that (7.2) is acceptable as a sufficient stability condition for shallow shells. But it turns out [55] that in non-linear 3-D elasticity theory the required Fréchet derivatives generally do not exist for reasonable choices of norm and strain energy.

This means that  $\Delta \phi$  and  $\delta^2 \phi$  need not share the same sign, no matter how small  $\|\delta u\|$  is made. A striking example given by Koiter [56] displays a very simple regular functional  $\phi[u(x)]$  for which  $\delta^2 \phi$  is positive in the sense of (7.2), but for which  $\Delta \phi$  can be made negative for arbitrarily small norm  $\|u\| = \left[ \int_0^1 (u^2 + u_x^2) dx \right]^{1/2}$ .

What is to be done about this? Koiter's counterexample involved very tortured deformation states with huge second derivatives, and this evidently gave him the successful idea of salvaging the second-variation criterion by introducing a modified strain-energy functional that depends on strain gradients as well as strains [56]. Despite Koiter's later [2] lack of enthusiasm for this device, it remains fairly persuasive as an argument for the *practical* reliability of the second-variation criterion. Another pragmatic viewpoint that one might adopt is to note that regular potentials of finite-dimensional systems have Fréchet derivatives of all order, and invoke a presumption of the accuracy of finite-element approximations.

But there is no doubt that at least an esthetic problem remains, and that a new, congenial definition of stability is desirable. Perhaps some statistical concepts may be fruitful. When the second-variation method fails, it appears that the minimum in  $\phi$  is destroyed only by the presence of obscure secret passages in function space into which no self-respecting structure would venture except by wildly improbable accident. Accordingly, an appropriately defined *probability* of failure should, under these circumstances, be absurdly low. But we do not have any helpful suggestions concerning such a definition, which, in order to be useful in the assessment of the *practical* stability of a structure, should permit easy evaluation of the desired probability.

## 8. Concluding Remarks

Many very interesting recent buckling papers simply could not be mentioned in this survey, and we regret this; the subject is just too big. In particular, we have not mentioned current progress in experimentation, dynamic buckling, creep buckling, and numerical methods. Some wise comments concerning catastrophe theory might have been appropriate. But we happily leave these, and other topics, to the next surveyors, who, if past experience is any guide, are already preparing their reviews.

## Acknowledgement

This work was supported in part by the National Science Foundation under Grant NSF-MCS78-07598, and by the Division of Applied Sciences, Harvard University.

## References

1. Tvergaard, V., 'Buckling Behavior of Plate and Shell Structures', *Proc. 14th IUTAM Congress*, Delft, North-Holland, 233-247 (1976).
2. Koiter, W.T., 'Current Trends in the Theory of Buckling', *Proc. IUTAM Symp. on Buckling of Structures*, 1974 (Ed. B. Budiansky), Springer-Verlag, 1-16 (1976).
3. Budiansky, B., 'Theory of Buckling and Post-Buckling Behavior of Elastic Structures', in *Advances in Applied Mechanics*, Vol. 14, Academic Press, 1-65 (1974).
4. Koiter, W.T., *Over de stabiliteit van het elastisch evenwicht*, Thesis, Delft, H.J. Paris, Amsterdam (1945). English transl. (a) NASA TT-F10, 833 (1967) (b) AFFDL-TR-70-25 (1970).
5. Budiansky, B. and Hutchinson, J.W., 'Dynamic Buckling of Imperfection-Sensitive Structures', *Proc. 11th IUTAM Congress*, Munich, 636-651 (1964).
6. Sewell, M.J., 'A General Theory of Equilibrium Paths Through Critical Points', I, II, *Proc. Roy. Soc. A306*, 201-223, 225-238 (1968).
7. Thompson, J.M.T. and Hunt, G.W., *A General Theory of Elastic Stability*, Wiley, New York (1973).
8. Budiansky, B. and Hutchinson, J.W., 'A Survey of Some Buckling Problems', *AIAA J.*, 4, 1505-1510 (1966).
9. Hutchinson, J.W. and Koiter, W.T., 'Postbuckling Theory', *App. Mech. Rev.*, 23, 1353-1366 (1970).
10. Crawford, R.F. and Hedgepeth, J.M., 'Effects of Initial Waviness on the Strength and Design of Built-up Structures', *AIAA J.*, 13, 672-675 (1975).
11. van der Neut, A., 'The Interaction of Local Buckling and Column Failure of Thin-Walled Compression Members', *Proc. 12th IUTAM Congress*, Springer-Verlag, 389-399 (1969).
12. Meijer, J.J. and van der Neut, A., *The Interaction of Local Buckling and Column Failure of Imperfect Thin-Walled Compression Members*, Delft University of Technology, Rep. VTH-160 (1970).
13. van der Neut, A., 'The Sensitivity of Thin-Walled Compression Members to Column Axis Imperfection', *Int. J. Solids Structures*, 9, 999-1011 (1973).
14. Koiter, W.T. and Kuiken, G.D.C., *The Interaction Between Local Buckling and Overall Buckling on the Behavior of Built-up Columns*, Delft University of Technology, Rep. WTHD 23 (1971).
15. Tvergaard, V., 'Imperfection Sensitivity of a Wide Integrally Stiffened Panel Under Compression', *Int. J. Solids Structures*, 9, 177-192 (1973).
16. Tvergaard, V., 'Influence of Post-Buckling Behavior on Optimum Design of Stiffened Panels', *Int. J. Solids Structures*, 9, 1519-1534 (1973).
17. van der Neut, A., 'Mode Interaction with Stiffened Panels', *Proc. IUTAM Symp. on Buckling of Structures*, 1974 (Ed. B. Budiansky), Springer-Verlag, 117-132 (1976).
18. Koiter, W.T. and Pignataro, M., 'An Alternative Approach to the Interaction Between Local and Overall Buckling in Stiffened Panels', *Proc. IUTAM Symp. on Buckling of Structures*, 1974 (Ed. B. Budiansky), Springer-Verlag, 133-148 (1976).

19. Koiter, W.T. and Pignataro, M., *A General Theory for the Interaction Between Local and Overall Buckling of Stiffened Panels*, Delft University of Technology, Rep. WTHD 83 (1976).
20. van der Neut, A., *The Interaction of Local and Overall Buckling in Stiffened Panels*, Delft University of Technology, Rep. LR-255 (1977).
21. Byskov, E. and Hutchinson, J.W., 'Mode Interaction in Axially Stiffened Cylindrical Shells', *AIAA J.*, **15**, 941-948 (1977).
22. Koiter, W.T., *General Theory of Mode Interaction in Stiffened Plate and Shell Structures*, Delft University of Technology, Rep. WTHD 91 (1976).
23. Koiter, W.T. and van der Neut, A., *Interaction Between Local and Overall Buckling of Stiffened Compression Panels*, paper presented at Int'l. Conf. on Thin-Walled Structures, University of Strathclyde, April 3-6 (1979).
24. Williams, F.W., Wittrick, W.H. and Plank, R.J., 'Critical Buckling Loads of Some Prismatic Plate Assemblies', *Proc. IUTAM Symp. on Buckling of Structures*, 1974 (Ed. B. Budiansky), Springer-Verlag, 17-26, (1976).
25. Bushnell, D., 'Buckling of Elastic-Plastic Shells of Revolution with Discrete Elastic-Plastic Ring Stiffeners', *Int. J. Solids Structures*, **12**, 51-66 (1976).
26. Almroth, B.O., Meller, E. and Brogan, F.A., 'Computer Solutions for Static and Dynamic Buckling of Shells', *Proc. IUTAM Symp. on Buckling of Structures*, 1974 (Ed. B. Budiansky), Springer-Verlag, 52-65 (1976).
27. Shanley, F.R., 'Inelastic Column Theory', *J. Aero. Sci.*, **14**, 261-267 (1947).
28. Hill R., 'Bifurcation and Uniqueness in Nonlinear Mechanics of Continua', in Muskhelishvili Volume, *Soc. Ind. Appl. Math.*, Philadelphia, Pennsylvania, 95-102 (1961).
29. Sewell, M.J., 'A Survey of Plastic Buckling', in *Stability* (Ed. H. Leipholz), Univ. Waterloo Press, Ontario, 85-197 (1972).
30. Sewell, M.J., *Elastic and Plastic Bifurcation Theory*, Report of Dept. of Mathematics, University of Reading, England (July 1975).
31. Storåkers, B., *Uniqueness and Stability at Finite Deformation of Inelastic Solids*, Publication No. 186, Dept. of Strength of Materials and Solid Mechanics, Royal Inst. of Tech., Stockholm (April 1973).
32. Hutchinson, J.W., 'Plastic Buckling', in *Advances in Applied Mechanics*, Vol. 14, Academic Press, 67-144 (1974).
33. Hutchinson, J.W., 'Post-Bifurcation Behavior in the Plastic Range', *J. Mech. Phys. Solids*, **21**, 163-190 (1973).
34. Tvergaard, V. and Needleman, A., 'On the Buckling of Elastic-Plastic Columns with Asymmetric Cross-Sections', *Int. J. Mech. Sci.*, **17**, 419-424, (1975).
35. Tvergaard, V. and Needleman, A., 'Buckling of Eccentrically Stiffened Elastic-Plastic Panels on Two Simple Supports or Multiply Supported', *Int. J. Solids Structures*, **11**, 647-663 (1975).
36. van der Heijden, A.M.A., *A Study of Hutchinson's Plastic Buckling Model* (January 1979), to be published.
37. von Karman, Th., 'Untersuchungen über Knickfestigkeit, Mitteilungen über Forschungsarbeiten', *Ver. Deut. Ing. Forschungsh.*, **81** (1910).
38. Hutchinson, J.W., 'Imperfection-Sensitivity in the Plastic Range', *J. Mech. Phys. Solids*, **21**, 191-204 (1973).
39. Onat, E.T. and Drucker, D.C., 'Inelastic Instability and Incremental Theories of Plasticity', *J. Aero. Sci.*, **20**, 181-186 (1953).
40. Hutchinson, J.W. and Budiansky, B., 'Analytical and Numerical Study of the Effects of



- Initial Imperfections on the Inelastic Buckling of a Cruciform Column', *Proc. IUTAM Symp. on Buckling of Structures*, 1974 (Ed. B. Budiansky), Springer-Verlag, 95-105 (1976).
41. Needleman, A. and Tvergaard, V., 'An Analysis of the Imperfection-Sensitivity of Square Elastic-Plastic Plates under Axial Compression', *Int. J. Solids Structures*, **12**, 185-201 (1976).
  42. Sewell, M.J., 'A Plastic Flow Rule at a Yield Vertex', *J. Mech. Phys. Solids*, **22**, 469-490 (1974).
  43. Christoffersen, J. and Hutchinson, J.W., *A Class of Phenomenological Corner Theories of Plasticity*, Harvard University Report MECH-8 (January 1979).
  44. Batdorf, S.B., 'Theories of Plastic Buckling', *J. Aero. Sci.*, **16**, 405-408 (1949).
  45. Koiter, W.T. and Skaloud, M., comments in: Colloque sur le comportement postcritique des plaques utilisées en construction métallique, *Mem. Soc. Roy. d. Sciences de Liège*, **5**, VIII, 64-68, 103, 104 (1963).
  46. Libai, A., *On the Optimization of a Stiffened Square Panel under Buckling Constraints*, Harvard University Report DAS M-6 (December 1977).
  47. Schuette, E.H., *Charts for the Minimum-Weight Design of 245-T Aluminum-Alloy Flat Compression Panels with Longitudinal Z-Section Stiffeners*, NACA Report No. 827 (1945).
  48. Hickman, W.A. and Dow, N.F., *Compressive Strength of 245-T Aluminum-Alloy Flat Panels with Longitudinal Formed Hat-Section Stiffeners Having a Ratio of Stiffener Thickness to Skin Thickness Equal to 1.00*, NACA Techn. Note 1439 (1947).
  49. Amazigo, J.C., 'Buckling of Stochastically Imperfect Structures', *Proc. IUTAM Symp. on Buckling of Structures*, 1974 (Ed. B. Budiansky), Springer-Verlag, 172-182 (1976).
  50. Miller, R.K. and Hedgepeth, J.M., 'The Buckling of Lattice Columns with Stochastic Imperfections', *Int. J. Solids Structures*, **15**, 73-84 (1979).
  51. Koiter, W.T., 'A Basic Open Problem in the Theory of Elastic Stability', *Proc. IUTAM/IMU Symp. on Application of Methods of Functional Analysis to Problems of Mechanics*, Marseilles (1975).
  52. Como, M. and Grimaldi, A., 'Stability, Buckling and Post-Buckling of Elastic Structures', *Meccanica*, **4**, 254-268 (1975).
  53. Como, M. and Grimaldi, A., 'Stability Analysis of Structural Elastic Systems', *Proc. IUTAM Symp. on Variational Methods in the Mechanics of Solids*, 1978, Pergamon Press (to be published 1979).
  54. Koiter, W.T., 'A Sufficient Condition for the Stability of Shallow Shells', *Proc. Kon. Ned. Ak. Wet., Series B*, **70**, 367-375 (1967).
  55. Martini, R., 'On the Fréchet Differentiability of Certain Energy Functionals', *Proc. Kon. Ned. Ak. Wet., Series A*, **79**, 326-330 (1976).
  56. Koiter, W.T., 'The Energy Criterion of Stability for Continuous Elastic Bodies', I, II, *Proc. Kon. Ned. Ak. Wet., Series B*, **68**, 178-202 (1965).